Int J Adv Manuf Technol (2014) 70:2263–2274
DOI 10.1007/s00170-013-5418-7

ORIGINAL ARTICLE

On efficient phase II process monitoring charts

Muhammad Riaz · Saddam Akber Abbasi · Shabbir Ahmad · Babar Zaman

Received: 7 February 2012 / Accepted: 7 October 2013 / Published online: 17 November 2013

Abstract Control charts act as the most effective statistical process control (SPC) tools for the monitoring of manufacturing processes. In this study, we propose and investigate a set Shewhart-type variability control chart based on the utilization of auxiliary information for efficient phase II process monitoring. The design parameters of the proposals are derived under correlated setups for the monitoring of variability parameter. The properties of these charting structures are evaluated in terms of average run length and some other related measures. The performance abilities of these charts are compared with each other and also with some existing counterparts. The comparisons revealed that the proposed charts are very efficient at detecting shifts in the variability parameter and have the ability to perform better than the competing charts in terms of run length characteristics. We have also used real datasets to illustrate the application of the proposed structures in practical situations.

Keywords Average run length (ARL) · Control charts · Extra quadratic loss (EQL) · In-control · Out-of-control · Phase II · Performance Comparison Index (PCI) · Process monitoring

M. Riaz · S. A. Abbasi (✉)
Department of Mathematics and Statistics, King Fahad University of Petroleum and Minerals, Dhahran 31261, Saudi Arabia
e-mail: saddamabbasi@yahoo.com

S. A. Abbasi
e-mail: saddamaa@kfupm.edu.sa

S. Ahmad
Department of Mathematics, COMSATS Institute of Information Technology, Wah Cantt 47040, Pakistan

B. Zaman
King Khaled Eye Specialist Hospital, Riyadh, Saudi Arabia

1 Introduction

Process monitoring had been there in all the eras in one form or the other in order to differentiate between the two types of variations in the process output. These variations are classified in two main types, namely, natural (random) and unnatural (nonrandom). In the first quarter of the twentieth century, statistical process control (SPC) formally came into picture for process monitoring purposes. SPC helps in monitoring processes for their stability with respect to different parameters (like location, spread, proportion, and correlation) using different statistical techniques like control charts, check sheets, Pareto diagrams, and histograms. These process monitoring techniques are now referred to as the SPC toolkit.

Control chart is the most important tool in SPC kit that has wide application in the monitoring of process parameters. One of the popular categories of control charts is Shewhart's chart, which mainly targets larger shifts. The design structures of these types of charts mainly depend on study variable(s). Sometimes information is also available on certain auxiliary variable(s) that are correlated with the study variable. These variables may be useful to improve the performance ability of the charting structures. The auxiliary characteristic(s) may be available in different forms such as a property to be monitored (cf. Alt [9]), a crude but simple to obtain measurement on the process (cf. Singh and Mangat [46]), an early measurement in the process (cf. Shu et al. [43], Riaz and Does [36], Ahmad et al. [4, 6, 7] and the references therein).

The information on auxiliary variables [along with the quality characteristic(s) of interest] may be accessible at the stage of estimation, testing or monitoring. The most popular styles of taking benefit of auxiliary information are ratio, product, and regression-type estimators (cf. Fuller [15]). The estimators based on these approaches are designed such that they make use of the auxiliary information along with the study variable (characteristic of interest) that leads to a boost

Table 1 Control charting structures

Charts	Mean (m_i) and standard deviations (d_i)
$V_u=s_y^2$	$m_u=\sigma_y^2$ and $d_u=\sigma_y^2\sqrt{n^{-1}(\mu_{40}-1)}$
$V_r=s_y^2\frac{\sigma_x^2}{s_x^2}$	$m_r=\sigma_y^2[n^{-1}(\mu_{40}-\mu_{22})+1]$ and $d_r=\sigma_y^2\sqrt{n^{-1}[(\mu_{40}-1)+(\mu_{04}-1)-2(\mu_{22}-1)]}$
$V_g=s_y^2+b_{yx}(\sigma_x^2-s_x^2)$	$m_g=\sigma_y^2$ and $d_g=\sigma_y^2\sqrt{n^{-1}\left[(\mu_{40}-1)+(\mu_{04}-1)b_{yx}^2/R^2-2(\mu_{22}-1)b_{yx}/R\right]}$ where $R=\sigma_y^2/\sigma_x^2$ and $b_{yx}=R(\mu_{22}-1)/(\mu_{04}-1)$
$V_{pr}=s_y^2\left(\frac{\sigma_x^2}{s_x^2}\right)^{\rho_{yx}^2}$	$m_{pr}=\sigma_y^2\left[n^{-1}\left\{(\mu_{04}-1)\rho_{yx}^2\left(\rho_{yx}^2+1\right)/2-(\mu_{22}-1)\rho_{yx}^2\right\}+1\right]$ and $d_{pr}=\sigma_y^2\sqrt{n^{-1}\left[(\mu_{40}-1)+(\mu_{04}-1)\rho_{yx}^4-2(\mu_{22}-1)\rho_{yx}^2\right]}$
$V_{re}=s_y^2\exp\left(\frac{\sigma_x^2-s_x^2}{\sigma_x^2+s_x^2}\right)$	$m_{re}=\sigma_y^2[0.5n^{-1}(0.75\mu_{04}-\mu_{22}-0.25)+1]$ and $d_{re}=\sigma_y^2\sqrt{n^{-1}[(\mu_{40}-1)+0.25(\mu_{04}-1)-(\mu_{22}-1)]}$.
$V_{rg}=s_y^2\sigma_x^2/s_x^2+b_{yx}(\sigma_x^2-s_x^2)$	$m_{rg}=\sigma_y^2[n^{-1}\{(\mu_{04}-1)-(\mu_{22}-1)\}+1]$and $d_{rg}=\sigma_y^2n^{-1/2}\sqrt{\left[\begin{array}{l}\{(\mu_{40}-1)+(\mu_{04}-1)-2(\mu_{22}-1)\}+b_{yx}^2/R^2\\ \times(\mu_{04}-1)-2b_{yx}/R\{(\mu_{22}-1)-(\mu_{04}-1)\}\end{array}\right]}$
$V_{prg}=s_y^2\left(\sigma_x^2/s_x^2\right)^{\rho_{yx}^2}+b_{yx}\left(\sigma_x^2-s_x^2\right)$	$m_{prg}=\sigma_y^2\left[n^{-1}\rho_{yx}^2\left\{\rho_{yx}^2(\mu_{04}-1)-(\mu_{22}-1)\right\}+1\right]$ and $d_{prg}=\sigma_y^2n^{-1/2}\sqrt{\left[\begin{array}{l}\left\{(\mu_{40}-1)+\rho_{yx}^4(\mu_{04}-1)-2\rho_{yx}^2(\mu_{22}-1)\right\}+b_{yx}^2/R^2\\ \times(\mu_{04}-1)-2b_{yx}/R\left\{(\mu_{22}-1)-\rho_{yx}^2(\mu_{04}-1)\right\}\end{array}\right]}$
$V_{reg}=s_y^2\exp\left(\frac{\sigma_x^2-s_x^2}{\sigma_x^2+s_x^2}\right)+b_{yx}\left(\sigma_x^2-s_x^2\right)$	$m_{reg}=\sigma_y^2[0.5n^{-1}\{(\mu_{04}-1)-(\mu_{22}-1)\}+1]$ and $d_{reg}=\sigma_y^2n^{-1/2}\sqrt{\left[\begin{array}{l}\{(\mu_{40}-1)+0.25(\mu_{04}-1)-2(\mu_{22}-1)\}+b_{yx}^2/R^2\\ \times(\mu_{04}-1)-2b_{yx}/R\{(\mu_{22}-1)-0.5(\mu_{04}-1)\}\end{array}\right]}$

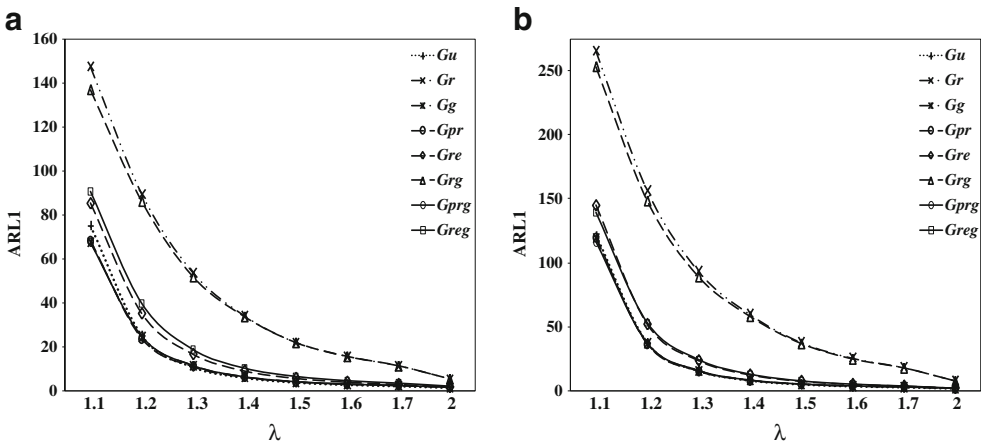

Fig. 1 **a** ARL curves of different charts for ARL_0=200, n=10, and ρ_{yx}=0.30. **b** ARL curves of different charts for ARL_0=371, n=10, and ρ_{yx}=0.30

in efficiency. There is a wide application of auxiliary information in different fields including agriculture, business, industry, health care, etc. In the quality control literature, the idea of exploiting correlation of the quality characteristic(s) of interest with some other associated quality characteristic(s) had been used by different researches.

The cause-selecting, regression-adjusted, and auxiliary information-based control charts are popular ways to capitalize the correlation between the study characteristic(s) and the concomitant characteristic(s). These approaches establish the dominance of the methods using information on additional characteristic(s). The literature in this direction may be seen in Mandel [27], Zhang [54, 55], Hawkins [20, 21], Wade and Woodall [50], Chen and Huang [11], Sheu and Tai [40], Riaz [33], Eyvazian et al. [13], Riaz [34, 35], Costa and Machado [12], Riaz and Does [36], Riaz et al. [37], Ahmad et al. [4, 7], Zhang et al. [56], and the references therein. This article is planned to propose the design structures of a set of Shewhart-type variability control chart, namely G_j charts, based on a correlated environment for phase II monitoring of variability parameter. We have used the information on auxiliary characteristic based on ratio, regression, power ratio, ratio exponential, and some of their mixed versions.

The organization of the rest of article is as: the design structures of the proposed control charts are given in Section 2, Section 3 contains the performance evaluations of the proposals and their comparisons with each other and with some existing counterparts using run length-based performance measures, Section 4 provides illustrative examples using real datasets showing the application of the proposed charting structures, and Section 5 summarizes and concludes the main findings of the study.

2 The proposed control charting structures

Let Y be the quality characteristic (which is the study variable) that is correlated with an auxiliary variable named X. The pairs (Y_i,X_i) for i=1, 2, 3, … are assumed to follow bivariate normal distribution with mean vector $\underline{\mu}$ and

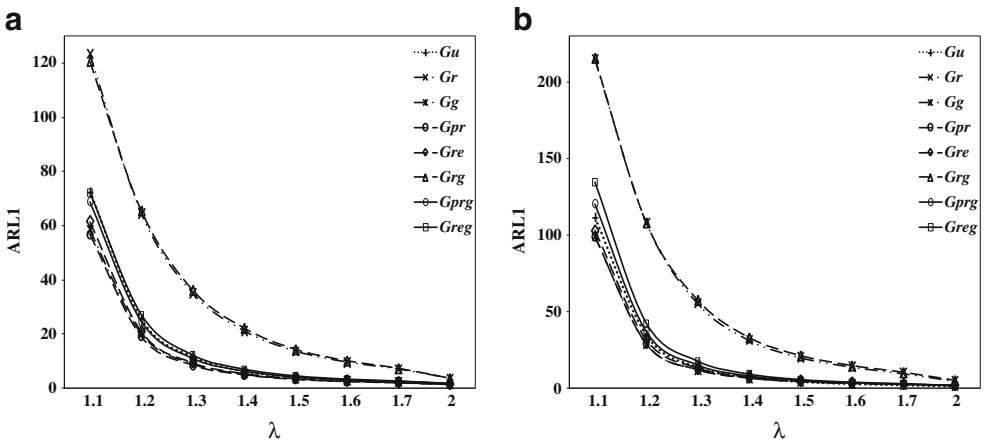

Fig. 2 **a** ARL curves of different charts for ARL_0=200, n=10, and ρ_{yx}=0.60. **b** ARL curves of different charts for ARL_0=371, n=10, and ρ_{yx}=0.60

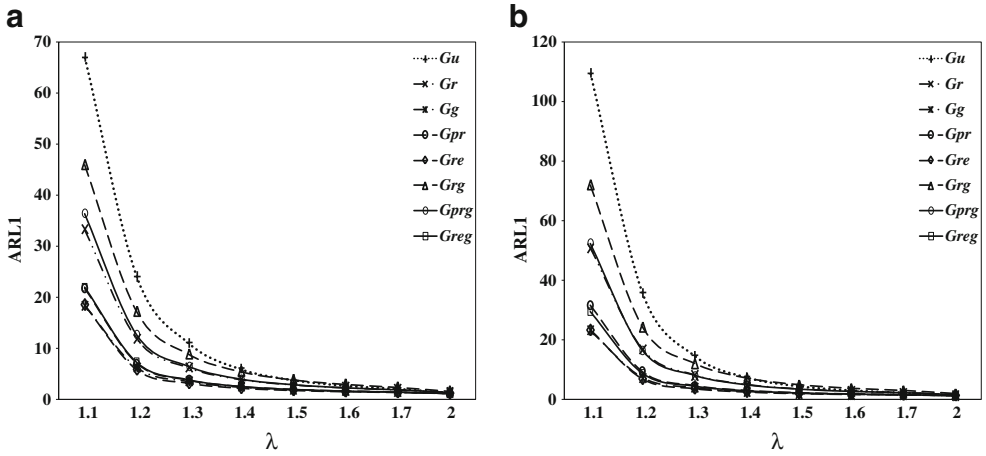

Fig. 3 **a** ARL curves of different charts for ARL_0=200, n=10, and ρ_{yx}=0.90. **b** ARL curves of different charts for ARL_0=371, n=10, and ρ_{yx}=0.90

variance–covariance matrix $\sum$. Symbolically, we may write as $(Y_i, X_i) \sim N_2(\underline{\mu}, \sum)$, where $\underline{\mu}$ and $\sum$ are defined as $\mu = (\mu_y, \mu_x)', \Sigma = \begin{pmatrix} \sigma_y^2 & \sigma_{yx} \\ \sigma_{xy} & \sigma_x^2 \end{pmatrix}$. Here, μ_y and μ_x are the in-control population means of Y and X, respectively; σ_y^2 and σ_x^2 are the population variances of Y and X respectively; $\sigma_{yx}=\sigma_{xy}$ is the covariance between Y and X. Moreover, the population correlation coefficient between Y and X is defined as $\rho_{yx}=\sigma_{yx}/\sigma_y\sigma_x$. It is to be mentioned that, in real situations, the information on the amount of correlation ρ_{yx} between the study variable Y and auxiliary variable X is generally available (cf. Garcia and Cebrian [16]); otherwise, we may estimate following Ahmed [8], Singh and Mangat [46], Yu and Lam [53], and Singh et al. [45].

Suppose (y_{1i}, x_{1i}), (y_{2i}, x_{2i}),(y_{3i}, x_{3i}), … (where i=1, 2, …, n) represent a sequence of paired observations of size n taken from (Y, X). Let $\bar{y}$ and $\bar{x}$ represent the sample means of Y and X, respectively; s_y^2 and s_x^2 and be the sample variances of Y and X, respectively, and b_{yx} is the amount of change in Y due to one unit change in X. Moreover, we assume $e_y=(s_y^2-\sigma_y^2)/\sigma_y^2$ and $e_x=(s_x^2-\sigma_x^2)/\sigma_x^2$ then we have $E(e_y)=E(e_x)=0$, $E(e_y^2)=n^{-1}(\mu_{40}-1)$,$E(e_x^2)=n^{-1}(\mu_{04}-1)$ and $E(e_xe_y)=n^{-1}(\mu_{22}-1)$ and where $\mu_{pq}=\frac{\eta_{pq}}{\sqrt{\eta_{20}^p\eta_{02}^q}}$ and $\eta_{pq}=E(y_i-\mu_y)^p(x_i-\mu_x)^q$ (cf. Srivastava and Jhajj [48], Singh [47], and Singh et al. [44]).

Based on these preliminaries, a set of variability estimators V_j ($\forall j=u,r,g,pr,re,rg,prg,$and reg) under simple random sampling (cf. Garcia and Cebrian [16], Upadhyaya and Singh [49], Kadilar and Cingi [23], and Ahmad et al. [7]) along with their means (m_j) and standard deviations (d_j) up to first order approximation are given in Table 1.

In order to establish a general structure based on V_j estimators, we define a quantity G as:

$$G_j = V_j/\sigma_y^2 \quad \forall \quad j = u, r, g, pr, re, rg, prg, \text{and } reg. \qquad (1)$$

It is to be mentioned that the distributional behavior of G_j depends on sample size for the estimator V_u and n and P_{yx} for

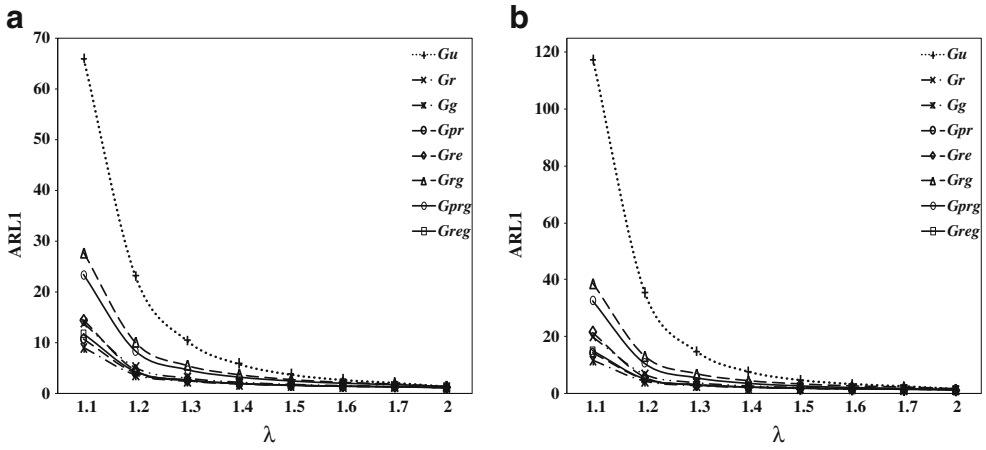

Fig. 4 **a** ARL curves of different charts for ARL_0=200, n=10, and ρ_{yx}=0.95. **b** ARL curves of different charts for ARL_0=371, n=10, and ρ_{yx}=0.95

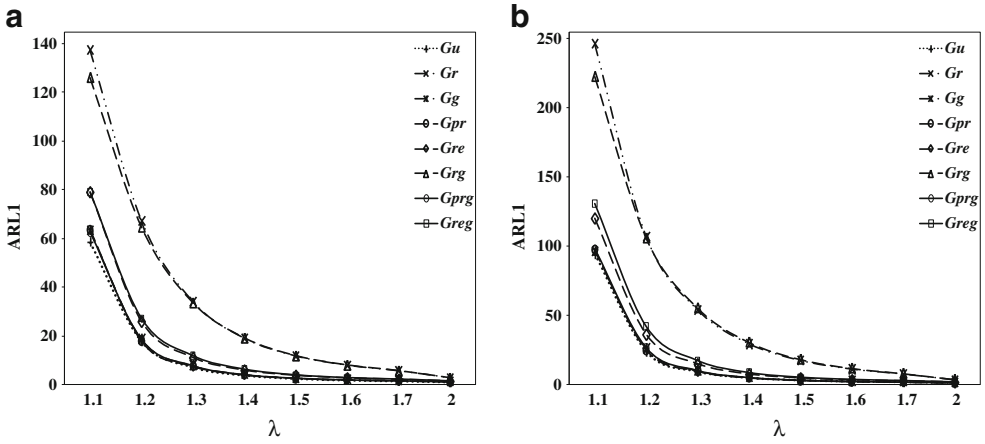

Fig. 5 **a** ARL curves of different charts for ARL_0=200, n=15, and ρ_{yx}=0.30. **b** ARL curves of different charts for ARL_0=371, n=15, and ρ_{yx}=0.30

other estimators. The analytical distributional results of one of the charting statistic, namely, G_r is provided in the Appendix, while for the others, one may work on the similar lines (although for some statistics, it may not be very straight forward).

Assume that the mean, standard deviation and αth quantile of generalized G_j charts are denoted by μ_{G_j}, σ_{G_j}, and G_{j_α} respectively (cf. Table 1). Based on these quantities, we can define the K-sigma and probability limits of G_j charts (using Shewhart's setup) as:

$$\left.\begin{array}{l} K-\text{sig limits} : \mathrm{LCL}_K = \mu_{V_j} - K\sigma_{V_j} \text{ and } \mathrm{UCL}_K = \mu_{V_j} + K\sigma_{V_j} \quad \forall j = u, r, \mathrm{g}, pr, re, rg, prg \text{ and } reg \\ \text{Prob limits} \quad : \mathrm{LCL}_P = V_{j_l} = G_{j_l}\sigma_y^2 \text{ with } F\left(G_j = G_{j_l}\right) \le \alpha_l \text{ and } \mathrm{UCL}_P = V_{j_u} = G_{j_u}\sigma_y^2 \text{ with } F\left(G_j = G_{j_u}\right) \ge 1-\alpha_u \end{array}\right\} \quad (2)$$

where $\alpha = \alpha_i + \alpha_u$ is probability of false alarm, F represents the cumulative distribution function and LCL,CL, and UCL refer to the lower control limit, central line, and upper control limit, respectively, of $\mathrm{G_j}(\forall_j = \mu, r, g, pr, re, rg, prg$, and $reg)$ charts.

Now, after defining the control limits using any of the structure given in Eq. (2) we use V_j ($\forall j = u, r, g, pr, re, rg, prg$, and reg) as the plotting statistic against their respective control limits. An out-of-control signal is received if any single point of the statistic V_j falls outside the corresponding limits given in Eq. (2), for phase II monitoring of process parameters based on future samples (prospective analysis). This decision rule is the most commonly used rule termed as one out of one. The other sensitizing rules (cf. Riaz et al. [38], Abbas et al. [2, 3], and Mehmood et al. [29]) may also be used with these proposed charting structures for more improved detection of process shifts.

It is to be mentioned that the correlated structures defined in this study may find applications in different fields such as radar systems, detection of noise signals, smoothing spectral quantities, etc. (cf. Lawson and Uhlenbeck [26] and Gerkmann and Martin [17] and the references therein). The performance abilities of such types of processes may be

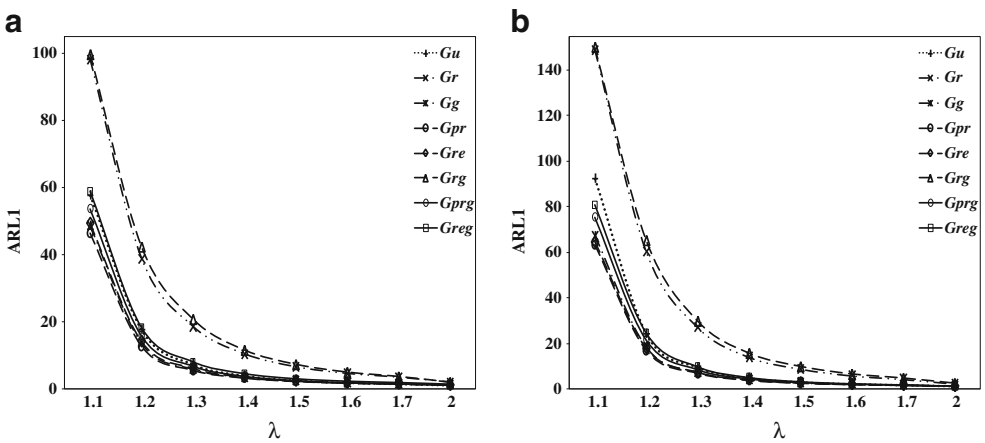

Fig. 6 **a** ARL curves of different charts for ARL_0=200, n=15, and ρ_{yx}=0.60. **b** ARL curves of different charts for ARL_0=371, n=15, and ρ_{yx}=0.60

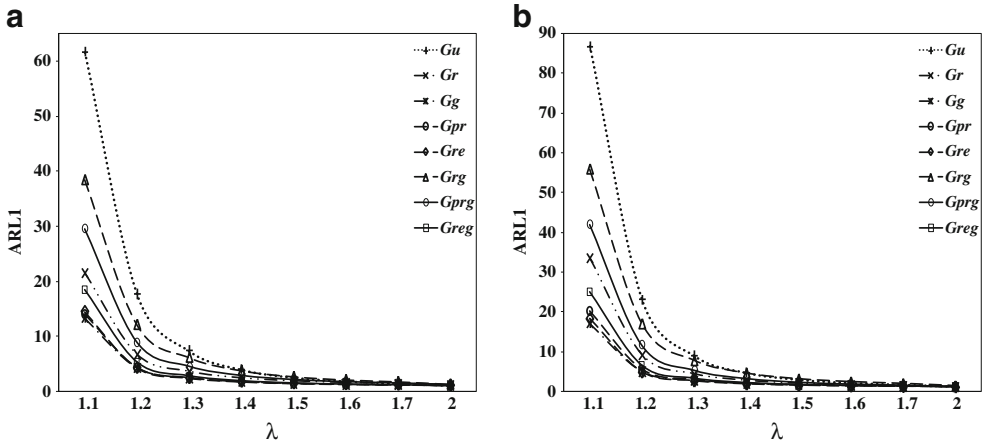

Fig. 7 **a** ARL curves of different charts for ARL_0=200, n=15, and ρ_{yx}=0.90. **b** ARL curves of different charts for ARL_0=371, n=15, and ρ_{yx}=0.90

improved with the suggested proposal of the study for an efficient monitoring of process parameters.

3 Performance evaluations and comparisons

This section evaluates the performance of the proposed G_j chart and provides some comparisons among each other and with some existing counterparts meant for the same purposes. To evaluate the performance of G_j charts for detecting shifts in phase II monitoring, we have considered the in-control value of process standard deviation as $\sigma_{y,0}$ and the out-of-control value as $\sigma_{y,1}$ defined as $\sigma_{y,1}=\lambda\sigma_{y,0}$, where λ represents the amount of shift. The performance measures used in this study include average run length (ARL), extra quadratic loss (EQL), relative average run length (RARL), and performance comparison index (PCI). The ARL measure is evaluated for each shift individually, while the other measures (EQL, RARL, and PCI) are evaluated over the whole range of λ values (from the smallest to the largest).

The ARL measure is defined as the number of samples before a false alarm is detected in the process. The measures EQL, RARL, and PCI are defined as (for the details on these measures see Wu et al. [51], Ou et al. [32], and Ahmad et al. [4, 7]:

$$\mathrm{EQL}=(\lambda_{\max}-\lambda_{\min})^{-1}\int_{\lambda_{\min}}^{\lambda_{\max}}\lambda^2 ARL(\lambda)\,d\lambda,\quad RARL=(\lambda_{\max}-\lambda_{\min})^{-1}\int_{\lambda\min}^{\lambda\max}\frac{\mathrm{ARL}(\lambda)}{\mathrm{ARL}_{\mathrm{bmk}}(\lambda)}\,\mathrm{d}\lambda \quad \text{and} \quad \mathrm{PCI}=\frac{\mathrm{EQL}}{\mathrm{EQL}_{\mathrm{bmk}}}$$

and where bmk refers to the benchmark chart (G_u chart is considered as benchmark chart in our study); ARL(λ) and $ARL_{bmk}(\lambda)$ are the average run lengths of a particular chart and the benchmark chart, respectively.

It is generally desirable to have larger values of ARL_0 (under in-control process) and smaller values of ARL_1 (under out-of-control process) for an efficient monitoring of process parameters. The EQL of an efficient chart attains minimum value similar to ARL. The measures RARL and PCI are equal to 1 for the benchmark chart; >1 for the inferior charts and <1 for superior charts.

To evaluate the performance of G_j charts, we have computed ARL values considering shifts in the standard deviation of Y, using probability limit approach given in Eq. (2), for specified ARL_0, n and P_{yx}. The ARL values are calculated for n=10 and 15 at some representative values of P_{yx} by fixing ARL_0=200 and 370 with λ=1 as in-control

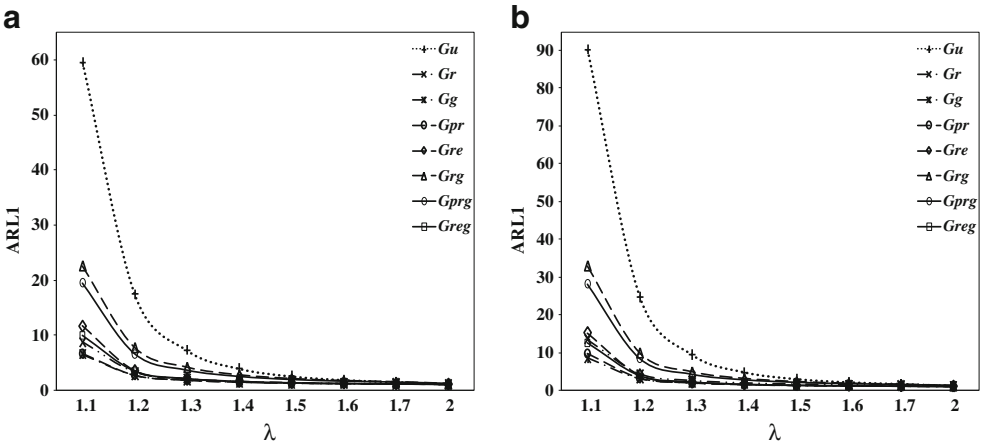

Fig. 8 **a** ARL curves of different charts for ARL_0=200, n=15, and ρ_{yx}=0.95. **b** ARL curves of different charts for ARL_0=371, n=15, and ρ_{yx}=0.95

Table 2 EQL, RARL, and PCI comparisons among G_j charts for ARL_0=200

Charts Choices	EQL	RARL	PCI	EQL	RARL	PCI	EQL	RARL	PCI	EQL	RARL	PCI
	P_{yx}=0.30 and n=10			P_{yx}=0.60 and n=10			P_{yx}=0.90 and n=10			P_{yx}=0.95 and n=10		
G_u	16.42	1.00	1.00	16.51	1.00	1.00	15.83	1.00	1.00	15.36	1.00	1.00
G_r	62.32	4.73	3.80	42.40	2.94	2.57	9.64	0.74	0.61	5.39	0.51	0.35
G_g	16.07	1.01	0.98	13.62	0.86	0.83	5.93	0.51	0.37	4.30	0.44	0.28
G_{pr}	15.71	0.99	0.96	13.18	0.84	0.80	6.59	0.55	0.42	4.58	0.46	0.30
G_{re}	22.08	1.40	1.35	14.36	0.91	0.87	5.66	0.49	0.36	4.89	0.46	0.32
G_{rg}	60.75	4.70	3.70	43.65	3.08	2.64	13.06	0.96	0.83	8.73	0.73	0.57
G_{prg}	16.10	1.02	0.98	15.97	0.98	0.97	10.01	0.75	0.63	7.50	0.64	0.49
G_{reg}	24.14	1.52	1.47	17.42	1.08	1.06	6.54	0.54	0.41	4.71	0.46	0.31
Choices	P_{yx}=0.30 and n=15			P_{yx}=0.60 and n=15			P_{yx}=0.90 and n=15			P_{yx}=0.95 and n=15		
G_u	11.93	1.00	1.00	11.89	1.00	1.00	12.20	1.00	1.00	11.96	1.00	1.00
G_r	40.94	3.74	3.43	24.67	2.17	2.08	6.14	0.69	0.50	3.96	0.55	0.33
G_g	12.59	1.04	1.06	10.00	0.88	0.84	4.56	0.57	0.37	3.52	0.51	0.29
G_{pr}	12.35	1.01	1.03	9.60	0.86	0.81	4.66	0.58	0.38	3.55	0.52	0.30
G_{re}	16.51	1.34	1.38	10.35	0.92	0.87	4.57	0.56	0.37	4.11	0.54	0.34
G_{rg}	39.95	3.75	3.35	26.71	2.40	2.25	9.60	0.96	0.79	6.80	0.77	0.57
G_{prg}	12.53	1.04	1.05	11.16	0.97	0.94	7.48	0.77	0.61	6.03	0.70	0.50
G_{reg}	17.10	1.40	1.43	12.46	1.07	1.05	5.26	0.61	0.43	4.02	0.54	0.34

value while $\lambda > 1$ as out-of-control value. The resulting values of ARL for G_j charts are compared graphically in the form of ARL curves in Figs. 1, 2, 3, 4, 5, 6, 7, and 8, where the ARL values are plotted y-axis versus λ values on x-axis. In order to evaluate the overall effectiveness of G_j charts, the EQL, RARL, and PCI values for same choice of ARL_0, n and P_{yx} are provided in Tables 2 and 3 for ARL=200 and 300, respectively. Moreover, same performance measures of some selective efficient control charts are compared with some existing control charts including NEWMA chart of Shu and Jiang [42], Improved R (IR) chart of Chen and Huang [11], synthetic R chart of Khoo and Lim [24], and the classical R

Table 3 EQL, RARL and PCI comparisons among G_j charts for ARL_0=371

Charts Choices	*EQL*	*RARL*	*PCI*	*EQL*	*RARL*	*PCI*	*EQL*	*RARL*	*PCI*	*EQL*	*RARL*	*PCI*
	P_{yx}=0.30 and n=10			P_{yx}=0.60 and n=10			P_{yx}=0.90 and n=10			P_{yx}=0.95 and n=10		
G_u	23.29	1.00	1.00	21.89	1.00	1.00	22.12	1.00	1.00	22.66	1.00	1.00
G_r	106.49	6.33	4.57	66.71	3.68	3.05	12.66	0.75	0.57	6.43	0.47	0.28
G_g	23.36	1.02	1.00	18.99	0.89	0.87	6.64	0.46	0.30	4.68	0.39	0.21
G_{pr}	22.93	0.99	0.98	19.04	0.90	0.87	8.04	0.52	0.36	5.16	0.41	0.23
G_{re}	31.94	1.44	1.37	20.42	0.97	0.93	6.33	0.44	0.29	5.74	0.41	0.25
G_{rg}	103.02	6.21	4.42	68.33	3.84	3.12	17.62	0.99	0.80	10.61	0.67	0.47
G_{prg}	23.12	1.01	0.99	23.28	1.05	1.06	12.46	0.72	0.56	9.02	0.59	0.40
G_{reg}	32.38	1.50	1.39	26.54	1.20	1.21	7.55	0.49	0.34	5.17	0.40	0.23
Choices	P_{yx}=0.30 and n=15			P_{yx}=0.60 and n=15			P_{yx}=0.90 and n=15			P_{yx}=0.95 and n=15		
G_u	16.02	1.00	1.00	16.07	1.00	1.00	15.36	1.00	1.00	16.07	1.00	1.00
G_r	64.65	4.70	4.04	35.50	2.46	2.21	7.81	0.71	0.51	4.62	0.52	0.29
G_g	16.85	1.04	1.05	12.57	0.86	0.78	5.00	0.54	0.33	3.80	0.48	0.24
G_{pr}	16.57	1.02	1.03	11.98	0.84	0.75	5.46	0.57	0.36	3.97	0.49	0.25
G_{re}	22.30	1.39	1.39	12.44	0.88	0.77	5.01	0.53	0.33	4.51	0.50	0.28
G_{rg}	63.77	4.80	3.98	38.03	2.71	2.37	12.33	0.99	0.80	8.20	0.74	0.51
G_{prg}	17.17	1.06	1.07	14.20	0.95	0.88	9.14	0.77	0.60	7.19	0.67	0.45
G_{reg}	25.01	1.54	1.56	15.75	1.05	0.98	6.05	0.59	0.39	4.36	0.50	0.27

Table 4 EQL, RARL, and PCI comparison of G_j charts with NEWMA, IR, Syn R, and classical R for $ARL_0=371$ and $n=10$

P_{yx}		0.30			0.60			0.90			0.95	
Charts	EQL	RARL	PCI	EQL	RARL	PCI	EQL	RARL	PCI	EQL	RARL	PCI
G_g	24.57	1.02	1.00	19.96	0.89	0.86	6.82	0.46	0.29	4.77	0.39	0.20
G_{pr}	24.13	0.99	0.99	20.03	0.89	0.87	8.30	0.52	0.36	5.26	0.41	0.22
NEWMA	17.14	0.81	0.70	17.14	0.83	0.74	17.14	0.82	0.74	17.14	0.82	0.72
IR	39.93	25.32	1.63	39.93	25.32	1.73	39.93	25.32	1.71	39.93	25.32	1.68
Syn R	11.40	7.06	0.47	11.40	7.06	0.49	11.40	7.06	0.49	11.40	7.06	0.48
R	22.26	14.01	0.91	22.26	14.01	0.96	22.26	14.01	0.96	22.26	14.01	0.93

chart (cf. Abbasi and Miller [1]) (cf. Table 4). It is to be mentioned that the smoothing parameter of NEWMA chart is taken as 1 for comparison purpose in our study.

It is to be mentioned that the ARL is obtained using Monte Carlo simulations with 10,000 iterations, while other measures are obtained by numerical integration method. Note that Kim [25] and Schaffer and Kim [39] indicate that even 5,000 replications are enough for finding ARLs in many control chart settings with in an acceptable error rate.

Following are the main findings of this study regarding the understudy G_j charts:

1. It is evident from Figs. 1, 2, 3, 4, 5, 6, 7, and 8 that the G_{pr} chart exhibited best performance followed by G_g, G_{prg}, G_{reg}, and G_{re} charts for low and moderate P_{yx}, while the G_g chart performs better than G_{pr} chart followed by G_{prg}, G_{reg}, and G_{re} charts for high value of P_{yx} in general.
2. As the value of P_{yx} increases, the performance of the G_j ($\forall j=r,g,pr,re,rg,prg,$and reg) charts gets keeps improving.
3. The most inferior performance is exhibited by G_r and G_{rg} for low and moderate values of P_{yx}, while the G_{rg} chart exhibited relatively lower performance for high values of P_{yx}.
4. The performance of proposed charts keep improving with an increase in the values of P_{yx}, n, and λ at a fixed ARL_0. Moreover, these structures remain ARL unbiased and monotonic irrespective of these choices.

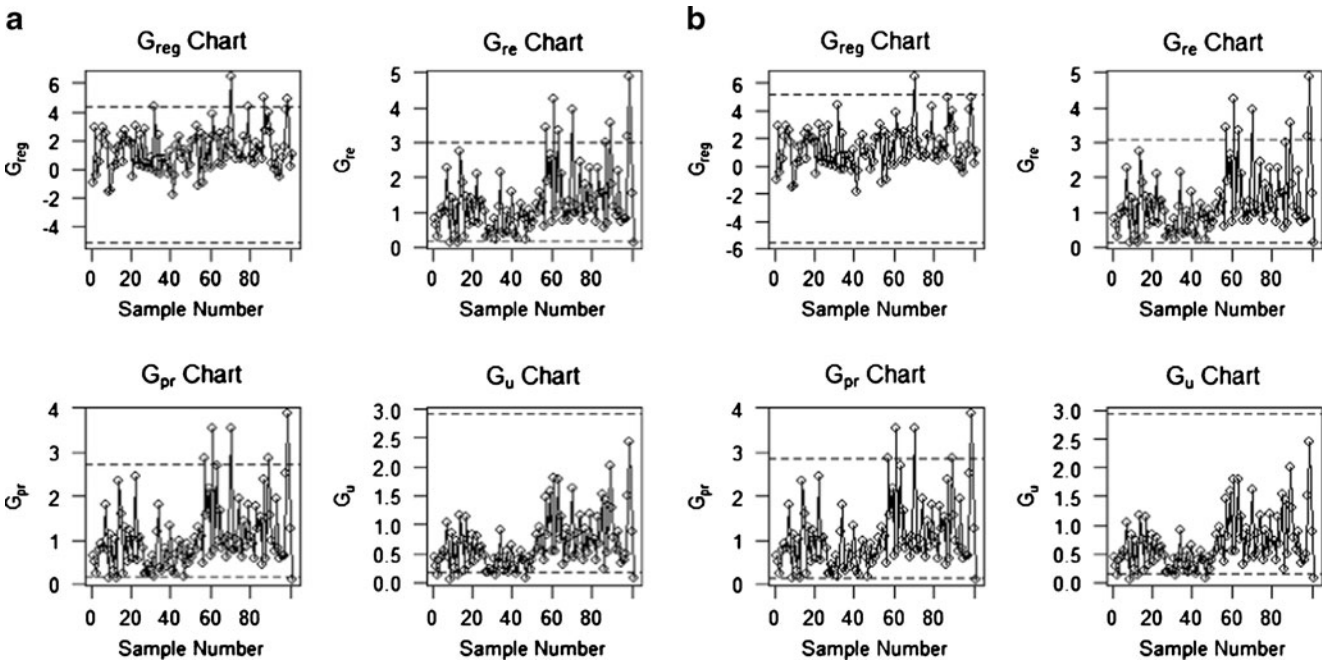

Fig. 9 **a** Control charts display of G_u, G_{pr}, G_{re}, and G_{reg} charts at $ARL_0=200$ and $n=10$. **b** Control charts display of G_u, G_{pr}, G_{re}, and G_{reg} charts at $ARL_0=371$ and $n=10$

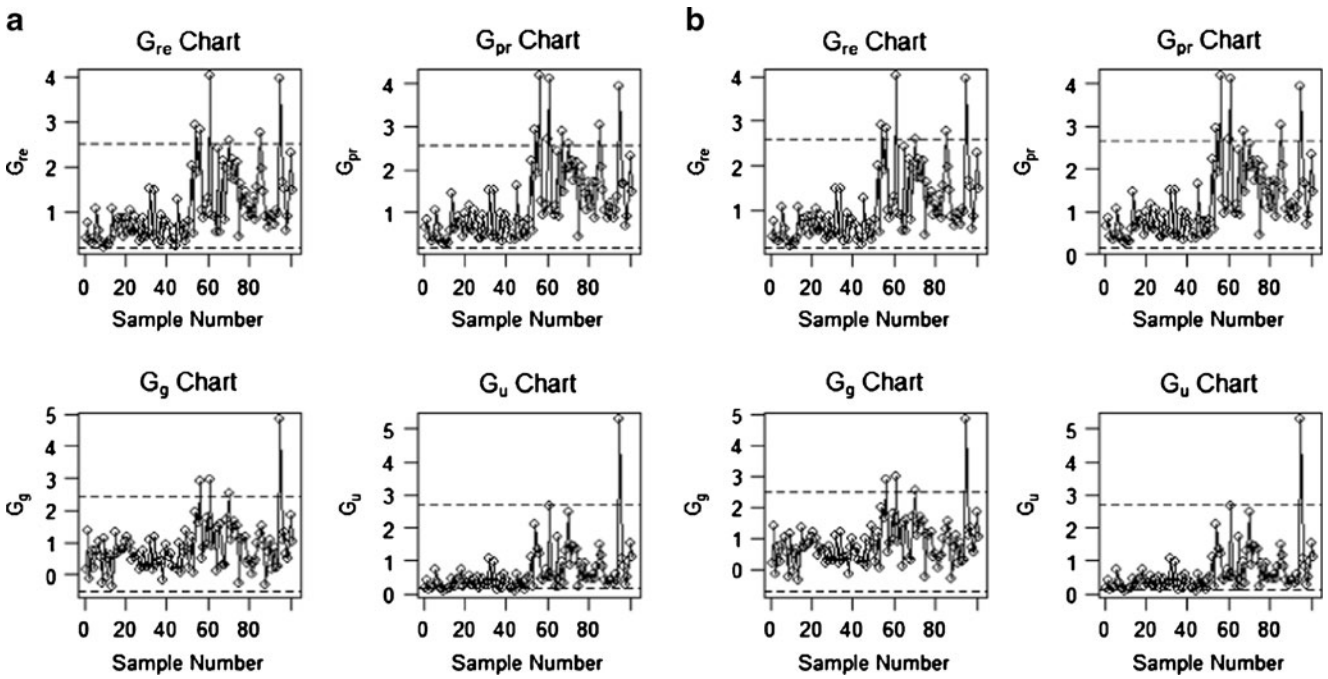

Fig. 10 **a** Control charts display of G_u, G_g, G_{pr}, and G_{re} charts at $ARL_0=200$ and $n=10$. **b** Control charts display of G_u, G_g, G_{pr}, and G_{re} charts at $ARL_0=371$ and $n=10$

5. The performance of proposed control charts keep improving with an increase in the values of P_{yx}, n, and λat a fixed ARL_0.
6. The performance of G_j charts in terms ARL is justified from the EQL, RARL, and PCI values provided in Tables 2 and 3 for $ARL_0=200$ and 500, respectively.
7. The efficient proposed charting sutures outperform the other existing counterparts, namely, NEWMA, IR, Syn R, and R charts particularly for higher correlation structures (cf. Table 4).

4 Illustrative example

In this section, we provide two examples to illustrate the practical application of auxiliary information based G_j ($\forall j = u, r, g, pr, re, rg, prg$, and reg) chats. Among G_i charts, we have considered G_u, G_g, G_{pr}, G_{re}, and G_{reg} charts, while the other charts may be considered in similar lines. The variables Y and X used for the construction of these charting statistics may be referred as: (1) to monitor the quality of pharmaceutical products, the units of pharmaceutical products may be considered as Y and the temperature in degrees Celsius may be considered as X; (2) to monitor the effective life of a cutting tool, Y: the life of tool, X: the tool angle, etc. Ahmad et al. [4, 5, 7], Riaz et al. [37], and Riaz and Does [36] gave many practical applications based on the use of auxiliary variables for process monitoring. The data set used in these examples is based on the nonisothermal continuous stirred tank chemical reactor model (namely, CSTR process) that has been widely used as benchmark by different authors, i.e., Marlin [28], Yoon and MacGregor [52], and Shi et al. [41].

Example 1: Based on G_u, G_{pr}, G_{re}, and G_{reg} charts—In this example, we consider outlet concentration of the production (C_A, kmol/m^3) as Y and flow rate of the solvent (F_S, m^3/min) as X. This bivariate data contains 1,024 values that have been collected on sampling interval of half minute. The first 512 values are in in-control state with shift ($\lambda=1$) in σ_y. For monitoring the process variability, we have introduced shift ($\lambda=1.5$) in σ_y (as $\sigma_1=\lambda\sigma_y=1.5\sigma_y$) of second half of data, where σ_0 and σ_1 represent the in-control and out-of-control standard deviations of Y, respectively. The said data set is considered in the form of 102 sub-groups each of size $n=10$ (by making each group after 5 min). The control limits for G_u, G_{pr}, G_{re}, and G_{reg} charts have been calculated at $ARL_0=200$ and $ARL_0=371$ The computed values of each charting statistic are displayed in the form of control charts by plotting sample number on horizontal axis and values of charting statistics on vertical axis (cf. Fig. 9a, b), respectively for $ARL_0=200$ and $ARL_0=371$, where the solid lines refer to the values of G_j ($\forall j = u, pr, re$, and reg) charts, while the dotted lines refer to the upper and lower control limits.

It is observed that the G_u, G_{pr}, G_{re}, and G_{reg} charts have detected 1, 6, 9, and 3 out-of-control signals, respectively (cf. Fig. 9a). It shows the superior detection ability G_{re} chart followed by G_{pr}, G_{reg}, and G_u charts, which is in accordance with the findings of Section 3. Similar type of performance order of G_u, G_{pr}, G_{re}, and G_{reg} charts can be observed in Fig. 9b.

Example 2: Based on G_u, G_g, G_{pr}, and G_{re} charts—In the example, we considered outlet temperature (T in Kelvin) as Y and cooling water temperature (T_C in Kelvin) as X. The control limits for G_u, G_g, G_{pr}, and G_{re} charts have been calculated and the resulting values of G_u, G_g, G_{pr}, and G_{re} charts are displayed in Figs. 3 and 4 for $ARL_0=200$ and $ARL_0=371$ in the form of control charts.

It is evident from Fig. 10a that G_u, G_g, G_{pr}, and G_{re} charts have detected 2, 4, 8, and 6 out-of-control signals, respectively. It shows that the best detection ability is offered by G_{pr} chart followed by G_u, G_g, and G_{re} charts. The similar behavior may be seen in Fig. 10b.

5 Summary, conclusions, and recommendations

Control charts are very effective tools to control and monitor the performance of any manufacturing or nonmanufacturing process. They have a range of variants for an improvement in their design structures in different styles. Auxiliary information-based control charts are very attractive alternatives to boost the performance ability of their design structures. This article presents different efficient control structures in the form of G_j charts (using different ways of using auxiliary information, including ratio, power ratio, ratio exponential, ratio regression, power ration regression, and ratio exponential regression) for phase II monitoring of the stability of process variability parameter. It is observed that the control charts based on regression (G_g) and power ratio (G_{pr}) charting statistics exhibited superior performance as compare to other charts in general. The G_{rg} chart expressed relatively lower performance as compare to other charting sutures in general. For the prospective analysis, the said design structures have the ability to perform better than many other existing variability charts like NEWMA, IR, Syn R, and R charts. The implementation of the proposed design structures with the practical data sets is very simple and attractive in timely receiving the out-of-control signals.

The scope of the proposal may also be extended by: incorporating the information on more auxiliary variables, implementing runs rules, investigating varying sampling strategies, and giving memory property to the proposed structures in the form of EWMA and CUSUM frames.

Acknowledgments Muhammad Riaz and Saddam Akber Abbasi are indebted to King Fahd University of Petroleum and Minerals (KFUPM), Dhahran, Saudi Arabia, for providing excellent research facilities. Muhammad Riaz would like to acknowledge the support provided by the Deanship of Scientific Research (DSR) at KFUPM for funding this work through project No. SB111008.

Appendix

Some distributional results: We define $M=s_y^2/s_x^2$ and $Q=\sigma_y^2/\sigma_x^2$; then, the joint probability density function of the random variables M and Q (the bivariate chi-square distribution obtained from the bivariate Wishart distribution) is given by:

$$f_{M,Q}(m,q)=\frac{(mq)^{(n-3)/2}}{2^{n-1}\,\Gamma^2((n-1)/2)(1-\rho^2)^{(n-1)/2}}\exp\left(-\frac{m+q}{2-2\rho^2}\right){}_0F_1\left[\frac{n-1}{2};\frac{\rho^2 mq}{(2-2\rho^2)^2}\right],$$

where $n>3$, $-1<\rho<1$ and ${}_0F_1\left[\frac{n-1}{2};\frac{\rho^2 mq}{(2-2\rho^2)^2}\right]$ is the hyper-geometric function as defined in Omar and Joarder [30]. Some more details in this regard may be seen in Gradshteyn and Ryzhik [18], Gunst and Webster [19], and Joarder [22]. For the case where $\rho=0$, the abovementioned joint density function of M and Q may be written as the product of two independent chi-square variables with $n-1$ degrees of freedom each. The probability density function of $G_r=M/Q$ is given as:

$$f_{V_\rho}(g_r)=\frac{2^{n-2}(1-\rho^2)^{(n-1)/2}}{B\left(\frac{1}{2},\frac{n-1}{2}\right)}\frac{g_r^{(n-3)/2}}{(1+g_r)^{n-1}}\left[1-\frac{4\rho^2 g_r}{(1+g_r)^2}\right]^{-n/2},\ g_r>0.$$

where $n>3$, $-1<\rho<1$ and $B\left(\frac{1}{2},\frac{n-1}{2}\right)$ represents the well known beta function. Omar and Joarder [30] named it as correlated F distribution which may have symbolic representation as $F(n-1,n-1,\rho)$. More details in this regard may be seen in Bose [10] and Finney [14].

The cumulative distribution function (Υ) of G_r is given as:

$$\Upsilon(g_r;n-1,n-1,\rho)=\frac{\Gamma(n-1)(1-\rho^2)^{(n-1)/2}}{\Gamma^2((n-1)/2)\Gamma(n/2)}\sum_{k=0}^{\infty}\Gamma\left(k+\frac{n}{2}\right)B\left(\frac{g_r}{1+g_r};k+\frac{n-1}{2};k+\frac{n-1}{2}\right)\frac{(4\rho^2)^k}{k!}$$

where Γ represents the gamma function, $n>3$ and $-1<\rho<1$. (cf. Omar et al. [31]).

The median point of the correlated $F(n-1,n-1,\rho)$ distribution given in Eq. (1) turns out to be 0.5 (cf. Omar and Joarder [30]). Moreover, there are three limiting distributional forms of $f_{G_r}(g_r)$ given as: when $n\to\infty$, $f_{G_r}(g_r)\to\text{Normal}(m_r,d_r)$; when $\rho\to0$, $f_{G_r}(g_r)\to F(n-1,n-1)$; when $\rho\to1$, $f_{G_r}(g_r)\to t_{n-1}$. (cf. Omar and Joarder [30]).

References

1. Abbasi SA, Miller A (2012) On proper choice of variability control chart for normal and non-normal processes. Qual Reliab Eng Int 28(3):279–296
2. Abbas N, Riaz M, Does RJMM (2011) Enhancing the performance of EWMA charts. Qual Reliab Eng Int 27(6):821–833
3. Abbasi SA, Riaz M, Miller A (2012) Enhancing the performance of CUSUM scale chart. Comput Ind Eng 63(2):400–409
4. Ahmad S, Lin Z, Abbasi SA, Riaz M (2012) On efficient monitoring of process dispersion using interquartile range. Open J Appl Sci 2:39–43
5. Ahmad S, Riaz M, Abbasi SA, Lin Z (2013) On median control charting under double sampling scheme. Eur J Ind Eng (in press)
6. Ahmad S, Riaz M, Abbasi SA, Lin Z (2013) On efficient median control charting. J Chin Inst Eng. doi:10.1080/02533839.02532013.02781794
7. Ahmad S, Riaz M, Abbasi SA, Lin Z (2013) On monitoring process variability under double sampling scheme. Int J Prod Econ 142(2):388–400
8. Ahmed SE (1992) Large sample pooling procedure for correlation. The Stat 41:415–428
9. Alt FB (1985) Multivariate quality control. Encycl Stat Sci 6:110–122
10. Bose SS (1935) On the distribution of the ratio of variances of two samples drawn from a given normal bivariate correlated population. Sankhya 2:65–72
11. Chen FL, Huang HJ (2005) A synthetic control chart for monitoring process dispersion with sample range. Int J Adv Manuf Technol 26(7–8):842–851
12. Costa A, Machado M (2009) A new chart based on sample variances for monitoring the covariance matrix of multivariate processes. Int J Adv Manuf Technol 41(7):770–779
13. Eyvazian M, Naini SGJ, Vaghefi A (2008) Monitoring process variability using exponentially weighted moving sample variance control charts. Int J Adv Manuf Technol 39(3–4):261–270
14. Finney DJ (1938) The distribution of the ratio of the estimates of the two variances in a sample from a bivariate normal population. Biometrika 30:190–192
15. Fuller WA (2009) Sampling statistics. Wiley, Hoboken
16. Garcia M, Cebrian A (1996) Repeated substitution method: the ratio estimator for the population variance. Metrika 43(1):101–105
17. Gerkmann T, Martin R (2009) On the statistics of spectral amplitudes after variance reduction by temporal cepstrum smoothing and cepstral nulling. IEEE Trans Signal Proc 57(11):4165–4174
18. Gradshteyn IS, Ryzhik IM (1994) Table of integrals, series and products. Academic, New York
19. Gunst RF, Webster JT (1973) Density functions of the bivariate chi-square distribution. J Stat Comput Simul 2:275–288
20. Hawkins DM (1991) Multivariate quality control based on regression-adjusted variables. Technometrics 33(1):61–75
21. Hawkins DM (1993) Regression adjustment for variables in multivariate quality control. J Qual Technol 25(3):170–182
22. Joarder AH (2009) Moments of the product and ratio of two correlated chi-square random variables. Statistical Papers 50(3):581–592
23. Kadilar C, Cingi H (2005) A new estimator using two auxiliary variables. Appl Math Comput 162(2):901–908
24. Khoo MBC, Lim EG (2005) An improved R (range) chart for monitoring the process variance. Qual Reliab Eng Int 21(1):43–50
25. Kim MJ (2005) Number of replications required in control chart Monte Carlo simulation studies. PhD Dissertation, University of Northern Colorado
26. Lawson JL, Uhlenbeck GE (1950) Threshold Signals. McGraw-Hill Book Co.
27. Mandel BJ (1969) The regression control chart. J Qual Technol 1:1–9
28. Marlin TE (ed) (2000) Process control: designing processes and control systems for dynamic performance (2 edn). McGraw-Hill, New York
29. Mehmood R, Riaz M, Does RJMM (2013) Efficient power computation for R out of M runs rules schemes. Comput Stat 28:667–381
30. Omar MH, Joarder AH (2011) Some moment characteristics of the ratio of correlated sample variances. Technical report no. 4223, Department of Mathematical Sciences, King Fahd University of Petroleum and Minerals
31. Omar MH, Joarder AH, Riaz M (2011) The cumulative distribution function of the ratio of correlated sample variances. Technical Report 422 (June 2011), Department of Mathematics and Statistics, KFUPM, Saudi Arabia
32. Ou YJ, Wu Z, Tsung F (2012) A comparison study of effectiveness and robustness of control charts for monitoring process mean. Int J Prod Econ 135(1):479–490
33. Riaz M (2007) On improved monitoring of process variability. Interstat 1
34. Riaz M (2008) Monitoring process mean level using auxiliary information. Statistica Neerlandica 62(4):458–481
35. Riaz M (2008) Monitoring process variability using auxiliary information. Comput Stat 23(2):253–276

36. Riaz M, Does RJMM (2009) A process variability control chart. Comput Stat 24(2):345–368
37. Riaz M, Mehmood R, Ahmad S, Abbasi SA (2013) On the performance of auxiliary based control charting under normality and non-normality with estimation effects. Qual Reliab Eng Int. doi:10.1002/qre.1467
38. Riaz M, Mehmood R, Does RJMM (2011) On the performance of different control charting rules. Qual Reliab Eng Int 27(8):1059–1067
39. Schaffer JR, Kim MJ (2007) Number of replications required in control chart Monte Carlo simulation studies. Commun Stat Simul Comput 36(5):1075–1087
40. Sheu SH, Tai SH (2006) Generally weighted moving average control chart for monitoring process variability. Int J Adv Manuf Technol 30(5–6):452–458
41. Shi X, Lv Y, Fei Z, Liang J (2013) A multivariable statistical process monitoring method based on multiscale analysis and principal curves. Int J Innov Comput Inf Control 9(4):1781–1800
42. Shu L, Jiang W (2008) A new EWMA chart for monitoring process dispersion. J Qual Technol 40(3):319–331
43. Shu L, Tsung F, Tsui KL (2005) Effects of estimation errors on cause-selecting charts. IIE Trans 37(6):559–567
44. Singh HP, Tailor R, Singh S, Kim JM (2011) Estimation of population variance in successive sampling. Qual Quant 45(3):477–494
45. Singh HP, Upadhyaya LN, Chandra P (2004) A general family of estimators for estimating population mean using two auxiliary variables in two-phase sampling. Stat Transit 6(7):1055–1077
46. Singh R, Mangat NS (1996) Elements of survey sampling. Kluwer, Dordrecht
47. Singh S (1991) Estimation of finite population variance using double sampling. Aligarh J Stat 11:53–56
48. Srivastava SK, Jhajj HS (1987) Improved estimation in two phase and successive sampling. J Indian Stat Assoc 25:71–75
49. Upadhyaya LN, Singh HP (2001) Estimation of the population standard deviation using auxiliary information. Am J Math Manag Sci 21:345–358
50. Wade MR, Woodall WH (1993) A review and analysis of cause-selecting control charts. J Qual Technol 25:161–169
51. Wu Z, Jiao JX, Yang M, Liu Y, Wang ZJ (2009) An enhanced adaptive CUSUM control chart. IIE Trans 41(7):642–653
52. Yoon S, MacGregor JF (2001) Fault diagnosis with multivariate statistical model Part I: using steady state fault signatures. J Process Control 11:387–400
53. Yu PLH, Lam K (1997) Regression estimator in ranked set sampling. Biometrics 53(3):1070–1080
54. Zhang GX (1984) A new type of control charts and a theory of diagnosis with control charts. World Quality Congress Transactions, American Society for Quality Control, London, pp 175–185
55. Zhang GX (1985) Cause-selecting control charts a new type of quality control charts. QR J 12(1):21–25
56. Zhang J, Li Z, Wang Z (2012) A new adaptive control chart for monitoring process mean and variability. Int J Adv Manuf Technol 60(9–12):1031–1038